This manuscript is textually identical with the published paper:

Borza P, Huber T, Leitner P, Remund N, Graf W (2018): Niche differentiation among invasive Ponto-Caspian *Chelicorophium* species (Crustacea, Amphipoda, Corophiidae) by food particle size. Aquatic Ecology 52(2): 179-190. DOI: 10.1007/s10452-018-9653-8

The original publication is available at:

http://link.springer.com/article/10.1007/s10452-018-9653-8

Niche differentiation among invasive Ponto-Caspian *Chelicorophium* species (Crustacea, Amphipoda, Corophiidae) by food particle size

Péter Borza[1,2*], Thomas Huber[3], Patrick Leitner[3], Nadine Remund[4], Wolfram Graf[3]

[1]GINOP Sustainable Ecosystems Group, MTA Centre for Ecological Research, Klebelsberg Kuno utca 3, H-8237 Tihany, Hungary

[2]Danube Research Institute, MTA Centre for Ecological Research, Karolina út 29-31, H-1113 Budapest, Hungary

[3]Department of Water, Atmosphere & Environment, Institute for Hydrobiology & Water Management, BOKU - University of Natural Resources and Applied Life Sciences, Gregor Mendel Strasse 33, A-1180 Vienna, Austria

[4]Info fauna – CSCF, Passage Maximilien-de-Meuron 6, CH-2000 Neuchâtel, Switzerland

[*] E-mail: borza.peter@okologia.mta.hu, tel: +361-279-3100/306

Acknowledgements

Joint Danube Survey 3 was organized by the International Commission for the Protection of the Danube River (ICPDR). We would like to thank everyone involved in the organization, field work, and evaluation of the survey for their effort, and Zsuzsanna Trábert for her assistance during the microscopy. This work was supported by the MARS project (Managing Aquatic ecosystems and water

Resources under multiple Stress) funded by the European Union under the 7th Framework Programme, grant agreement no: 603378, and the Economic Development and Innovation Operational Programme (GINOP) 2.3.2-15-2016-00019 grant. Péter Borza was supported by the Scholarship of the Scholarship Foundation of the Republic of Austria for Post-docs from October 2013 until March 2014 (funding organization: Österreichischer Austauschdienst GmbH on behalf of and financed by the Scholarship Foundation of the Republic of Austria).

Abstract

After *Chelicorophium curvispinum*, two other Ponto-Caspian tube-dwelling, filter feeding amphipod species (*C. robustum* and *C. sowinskyi*) have colonized several catchments in Central and Western Europe in recent decades. To reveal the mechanism of niche differentiation among them, we measured the mesh sizes of their filtering apparatus and analyzed multi-habitat sampling data from the River Danube using RDA-based variance partitioning between environmental and spatial explanatory variables. Morphometric data showed clear differentiation among the species by filter mesh size (*C. curvispinum* > *C. robustum* > *C. sowinskyi*). Field data also indicated the relevance of suspended matter; however, the mere quantity of suspended solids included in the analysis could not explain the abundance patterns effectively. Current velocity, substrate types, and total nitrogen content also had a non-negligible effect; however, their role in the niche differentiation of the species is not evident. In summary, differences in their filter mesh sizes indicate a niche differentiation by food particle size among the invasive *Chelicorophium* species, allowing their stable coexistence given sufficient size variability in their food source. Consequently, the two recent invaders increase the effectiveness of resource utilization, resulting in a more intensive benthic-pelagic coupling in the colonized ecosystems.

Keywords

benthic-pelagic coupling, filter feeding, invasion impact, River Danube, suspended matter

57

58 Introduction

59

60 Suspension feeding organisms play a key role in aquatic ecosystems by linking the pelagic and benthic
61 compartments of the food web (Atkinson et al. 2013; Zhang et al. 2016; Griffiths et al. 2017).
62 Accordingly, the establishment of a filter feeding invader can induce profound changes in the
63 functioning of both running and still waters (Sousa et al. 2014), well exemplified by the invasion
64 impact of the Ponto-Caspian dreissenid mussels, implying reduced plankton biomass, increased water
65 clarity favoring benthic algae and macrophytes, cyanobacterial blooms, increased benthic invertebrate
66 biomass, and consequent changes in fish assemblages (Higgins and Vander Zanden 2010).
67 The tube-dwelling euryhaline amphipods of the Ponto-Caspian *Chelicorophium* genus are also
68 suspension feeders, receiving attention mainly on account of their successful range expansion in
69 several Central and Western European catchments since the early 20th century. *Chelicorophium*
70 *curvispinum* (G.O. Sars, 1895), the first species of the genus to arrive in Western Europe (Bij de Vaate
71 et al. 2002) had a dramatic impact on the colonized waters, especially in the eutrophic River Rhine.
72 Here, the species reached extreme high densities in the 1980-90s (Van den Brink et al. 1993), and
73 formed a thick layer of muddy tubes on hard substrates which suffocated adult *Dreissena* mussels and
74 prevented the settlement of their larvae, resulting in the decline of the population (Van der Velde et al.
75 1994). At the same time, the species became an important food source for fish (Kelleher et al. 1998).
76 Although its abundance had decreased in the Rhine by the 2000s, presumably due to increased
77 predation pressure after the invasion of *Dikerogammarus villosus* (Sowinsky, 1894) (Van Riel et al.
78 2006), the species continues to be a key member of benthic macroinvertebrate assemblages in most
79 invaded waters (Noordhuis et al. 2009; Hellmann et al. 2015).
80 Recently, two additional representatives of the genus extended their ranges in Central and Western
81 Europe using the Danube-Rhine system. *Chelicorophium robustum* (G.O. Sars, 1895) – formerly
82 present in the Danube only downstream of the Serbian river section – was recorded in the River Main
83 in 2000 (Bernerth et al. 2005). It colonized the Upper and Middle Danube later by downstream drift
84 (Borza et al. 2015), and recently it was found in the Rhine (Bernauer and Jansen 2006; Altermatt et al.

2014) as well as in several connected French waterways (Labat et al. 2011). The third species, *Chelicorophium sowinskyi* (Martynov, 1924) was found in the Middle Danube already in the 1910s (Borza 2011), and recent records confirmed its presence in Austria, Germany, France, and Switzerland, as well (Bernerth and Dorow 2010; Borza et al. 2010; Forcellini 2012; Altermatt et al. 2014).

Despite their key functional role in aquatic ecosystems, the ecology of the invasive *Chelicorophium* species has received little scientific attention so far. Consequently, the mechanism of niche differentiation among the three species – informative of how the two recent invaders modify the impact of *C. curvispinum* – has not been revealed. Benthic filter feeding species usually compete for food or space (Svensson and Marshall 2015). In the former case, niche differentiation is achieved through partitioning of food sources by particle size (e.g. Lesser et al. 1992; Kang et al. 2009), while in the latter case the species show spatial separation along certain environmental factors, such as substrate properties, current velocity, or water depth (e.g. Brönmark and Malmqvist 1982; Jones and Ricciardi 2005). The two factors cannot be separated in all instances; e.g. hydropsychid caddisflies with larger filter mesh sizes tend to occur in microhabitats with stronger currents (Wallace et al. 1977). In the present study we aimed to reveal the mechanism of niche differentiation among the invasive *Chelicorophium* species by focusing on the two most likely factors. First, we examined whether differences can be observed in the mesh sizes of the filtering apparatus of the three species, suggesting niche differentiation by food particle size. Second, we tested whether certain environmental variables indicate spatial niche differentiation.

Material and methods

Morphometric data

We measured the filter mesh size of the invasive *Chelicorophium* species on microscopic dissections from specimens collected in the Lower Danube, where all three species occur natively (see 'Field data' for details on the sampling). Since abundant materials of all three species – allowing the representation

of their full body size spectrum in both genders – were not available from the same site, we included specimens from a site where the three species were present in similar density (river km 104, Sf. Gheorghe arm of the delta), and supplemented the material from sites where the species were abundant (river km 375 for *C. curvispinum* and *C. robustum*, and river km 532 for *C. sowinskyi*; Table 1).

The filter of corophiids is formed by two rows of plumose setae on the anterior margin of the merus of the second gnathopod, where the mesh size is determined by the distance between bristles (Riisgård and Larsen 2010: 275, fig. 25-26). To get a clear view on the medially oriented bristles of the distal (apical) row of setae, we carefully removed the medial (subapical) row of setae using a sharp pin under stereomicroscope. We then mounted the detached limbs on a slide and took digital photographs under light microscope with 100-fold magnification. Since the length of bristles appeared to increase toward the end of the setae and the distances between them increased accordingly, we took pictures of the relatively short and densely arranged basal bristles, the distances of which were assumed to provide a good approximation the filtered particle sizes (the long distal bristles can lean in the current, so the actual distances between them might be smaller). To diminish measurement error, we measured the distance between five bristles, which might imply a slight underestimation of the within-individual variation of filter mesh sizes (presented here as the distance between the centers of two neighboring bristles in μm). We made ten independent (i.e. non-overlapping) measurements on each specimen using the tpsdig 2.22 digital picture analysis software (Rohlf 2015).

Field data

The field samples analyzed in the present study were collected during the Joint Danube Survey 3 (13 August–26 September 2013) at 55 sites of the river between Ulm (river km 2,581) and the Delta (river km 18, Kiliya branch; Fig. 1) by the 'multi-habitat' approach based on, but not strictly following the AQEM protocol (Hering et al. 2004). At each site, 4-7 samples (altogether 251) consisting of five pooled units covering 25 x 25 cm bottom area were collected in the littoral zone by hand net (aperture: 25 x 25 cm, mesh size: 500 μm), representing all available habitat types (Table 2). All samples were preserved in 4% formaldehyde solution in the field, and stored in 70% ethanol after sorting. Sorting

was facilitated by fractioning the material on a set of sieves (mesh sizes: 0.5, 2, 5, 10, and 20 mm). In some cases, two to 64-fold subsampling of the smallest one or two fractions was necessary due to the extremely high number of juvenile animals in the samples. *Chelicorophium* specimens (altogether 11,451 individuals) could be identified to species level above ~2 mm body length (9,282 ind.); unidentifiable juveniles were omitted. Depth (range: 0.1-1.2 m) and current velocity (0-0.37 m/s; measured at approx. 5 cm from the bottom using Marsh-McBirney Flo-Mate™ Portable Velocity Flow Meter Model 2000) were recorded for each subsample and averaged separately for each site. Conductivity (9.29-566.00 µS/cm), pH (7.89-8.43), dissolved O_2 (5.89-10.42 mg/l), dissolved organic carbon (1.59-7.63 mg/l), total nitrogen (0.52-3.37 mg/l), total phosphorus (0.02-0.11 mg/l), and chlorophyll-a concentration (0.10-18.77 µg/l) were measured at two points per site near the river banks, whereas the concentration suspended matter ('total suspended solids', TSS hereafter; 2.5-50.0 mg/l) was recorded at one point per site during the survey.

Statistical analysis

We modelled filter mesh sizes in two steps. First, for descriptive purposes, we fitted linear mixed-effects models on each species separately, including standard body length (measured between the tip of the rostrum and the tip of the telson), gender, and sampling site as fixed effects, and individuals as a random effect using the 'nlme' package (Pinheiro et al. 2016) in R 3.2.5 (R Core Team 2016). Following the recommendations of Zuur et al. (2009), we assessed the fit of the models including all explanatory variables and their interactions using diagnostic figures. We then fitted variance functions, if considerable heteroscedasticity was detected (the choice of the function was based on *AIC* and *BIC* scores; the simpler model was preferred in cases of contradiction between the two scores), and after that we omitted non-significant fixed effects step-by-step based on the *t*-statistic (juveniles were included only if 'gender' was omitted). We characterized the optimal models by the parameters as well as the marginal R^2 (fixed effects; $R^2_{GLMM(m)}$) and conditional R^2 (fixed and random effects; $R^2_{GLMM(c)}$) as defined by Nakagawa and Schielzeth (2013), calculated by the 'sem.model.fits' function in the

168 'piecewiseSEM' package (Lefcheck 2016). We interpret among-individual variance (=random effects)
169 as $R^2_{GLMM(c)} - R^2_{GLMM(m)}$, and within-individual (=residual) variance as $1 - R^2_{GLMM(c)}$.
170 Second, to test for interspecific differences, we fitted a linear mixed-effects model on the three
171 species, following the procedure as described for the single-species models. We did not include
172 variables which had proved non-significant in the single-species models..
173 We tested for spatial niche differentiation by variance partitioning between environmental and spatial
174 explanatory variables based on redundancy analysis (RDA), using the 'varpart' function in the 'vegan'
175 package (Oksanen et al. 2017). We used ln(x+1) and Hellinger-transformed (Legendre and Gallagher
176 2001) count data (individuals per sample) in the analysis, but we show ind./m^2 values in the results and
177 in figures for the sake of comparability. We modelled the spatial structure of the study using the
178 asymmetric eigenvector map (AEM) method (Blanchet et al. 2008a; Blanchet et al. 2011) allowing the
179 consideration of directional spatial processes, induced by the currents in our case. Since the locations
180 of the samples within sites were not recorded, we considered only sites, using river km distances (d_{ij})
181 weighted as $1/d_{ij}$ (conforming to Borza et al. 2017a), and replicated the values of the generated
182 spatial variables (AEM eigenfunctions) for all samples within each site. We excluded two sites (8
183 samples) in the two minor arms of the Danube delta (Sulina and Sf. Gheorghe) allowing the one-
184 dimensional representation of the study design including 152 samples from 46 sites (64 samples did
185 not contain *Chelicorophium* species, and 27 additional samples were omitted due to missing values).
186 We used the eigenfunctions both with positive and negative Moran's *I* values (modelling positive and
187 negative spatial autocorrelation, respectively) in the analysis, which was possible due to the fact that
188 we only had 45 (number of sites minus one) AEM eigenfunctions for 152 samples. We performed
189 forward selection (Blanchet et al. 2008b) on the environmental variables with two different adding
190 limits (P = 0.05 and 0.01; using the 'ordiR2step' function in the 'vegan' package) to provide more
191 insight into their importance, but we used only the wider set of variables (P = 0.05) in variance
192 partitioning. For this, we selected spatial variables with P = 0.05 adding limit, as well, and tested
193 variance partitions of interest by ANOVA with 9999 permutations. We present the effect of the
194 environmental variables based on their biplot scores in the model including both environmental and

195 spatial variables. We mapped the environmentally explainable fraction of variance (including the
196 overlap) as well as the only spatially explainable part (without the overlap) by plotting the fitted site
197 scores (= linear constraints; '*LC*' scores) of the first canonical axis in the corresponding RDA models
198 against river km after Legendre and Legendre (2012).
199
200 Results
201
202 Morphometric data
203
204 The largest mesh sizes were observed in *C. curvispinum* (6.33-18.35 μm; Fig. 2). The inclusion of
205 body length as a fixed variance weight was supported (Table S1), whereas the effects of 'gender',
206 'sampling site', and all interaction terms could be neglected (Table S2). Among-individual variance
207 was high and within-individual variation was also considerable, which resulted in a relatively weak
208 but statistically significant body length-dependency (Table 3).
209 The filter mesh size of *C. robustum* ranged between 4.68 and 13.02 μm, increasing asymptotically
210 with body length (Fig. 2). However, non-linear models did not provide a good fit due to the relatively
211 short saturation interval; therefore, we divided the dataset into two approximately linear parts by
212 maximizing the difference between the slopes of the two segments, which allowed comparability with
213 the other two species. Below 5.5 mm, mesh sizes showed a clear linear increase with body length
214 despite considerable among- and within-individual variation (Table 3), whereas the effects of 'gender',
215 'sampling site' and the interaction terms were not significant(Table S2). The inclusion of variance
216 functions in the model was not supported (Table S1). Above 5.5 mm, the effect of body length on
217 filter mesh size was not significant ($P = 0.152$). 'Gender' and 'sampling site' were not included in the
218 model due to the strongly unbalanced design (only females attained sizes larger than ~ 6 mm, and
219 large specimens were rare at river km 104), and the usage of variance functions was not necessary,
220 either (Table S1). Since fixed effects were not included in the model and among-individual variability
221 was moderate, most of the variation was attributable to within-individual differences (Table 3).

222 The filter mesh size of *C. sowinskyi* was the smallest among the three species, ranging between 2.64
223 and 6.87 μm (Fig. 2). The usage of body length as a fixed weight was supported (Table S1), as
224 variance increased considerably with the size of the animals. Filter mesh size showed a clear linear
225 increase with body length, and the interaction between body length and gender also proved significant
226 (0.28, $SE = 0.05$; $P<0.001$), reflecting the fact that males attained smaller body lengths but had a mesh
227 size range similar to females (the effects of 'sampling site' and the interaction terms could be
228 neglected; Table S2). However, for the sake of comparability with the other species, we included only
229 body length in the model shown in Table 3, indicating considerable among-individual, but relatively
230 low within-individual variation.
231 To allow a meaningful interspecific comparison of filter mesh sizes in spite of the considerable effect
232 of body length, we excluded specimens of *C. robustum* larger than 5.5 mm from the model involving
233 all three species. As the effects of 'gender', 'sampling site' and the interaction terms proved
234 insignificant in the single-species models (the body length-gender interaction was significant but
235 negligible compared to interspecific differences in *C. sowinskyi*) , they were not included in the initial
236 model. The usage of a stratified variance structure was supported (Table S1; parameters. *C.*
237 *curvispinum*: 1.20; *C. robustum*: 1; *C. sowinskyi*: 0.38). Body length showed negligible interactions
238 among the species ($P = 0.805$ for *C. curvispinum*, $P = 0.842$ for *C. sowinskyi*), so interspecific
239 differences in filter mesh size could be interpreted as the differences among the intercepts of the fitted
240 lines (fixed effects), which were estimated 2.86 μm ($SE = 0.37$; $P < 0.001$) between *C. curvispinum*
241 and *C. robustum*, and 3.52 μm ($SE = 0.40$; $P < 0.001$) between *C. robustum* and *C. sowinskyi* (Fig. 2).
242
243 Field data
244
245 Three *Chelicorophium* species were recorded during the survey of which *C. curvispinum* was the most
246 common, occurring at 51 sites (169 samples) between river km 2,415 and 18 (Fig. 1) with a maximum
247 density of 5,280 ind./m^2 (median: 42, interquartile range: 10-208; zeros not included). *C. sowinskyi*
248 was found between river km 2,415 and 18 during the survey (38 sites, 106 samples); however, it was
249 missing between river km 1,630 and 1,199 (Fig. 1). It reached extreme high densities (54,835 and

250 43,904 ind./m^2) in two samples taken below the mouth of the River Jantra (river km 532), whereas in
251 other parts of the river its density did not exceed 5,050 ind./m^2 (median: 37, interquartile range: 10-
252 112 including the two extreme values). *C. robustum* was recorded at 37 sites (89 samples) between
253 river km 2,415 and 26 with a notable gap between river km 1,367 and 1,159 (Fig. 1). The highest
254 density of the species was 5,523 ind./m^2 (median: 16, interquartile range: 3-64).
255 The forward selection procedure with $P = 0.05$ adding limit selected TSS, substrate type, current
256 velocity, and total nitrogen concentration of the environmental variables which altogether explained
257 22.7% ($df = 13$, $F = 4.40$, $P < 0.001$) of the total variation, whereas the nineteen selected AEM
258 eigenfunctions accounted for 43.1% ($df = 19$, $F = 7.01$, $P < 0.001$). The overlap between the two
259 variance portions was considerable (16.0%; not testable), hence 6.7% ($df = 13$, $F = 2.35$, $P < 0.001$)
260 and 27.1% ($df = 19$, $F = 4.91$, $P < 0.001$) could be explained exclusively by environmental and spatial
261 variables, respectively. The two variable sets together accounted for 49.7% ($df = 32$, $F = 5.67$, $P <$
262 0.001) of the total variation. With $P = 0.01$ adding limit, the only selected environmental variable was
263 TSS, explaining 13.3% alone ($df = 1$, $F = 24.14$, $P < 0.001$).
264 The Mantel correlogram (Fig. 3) revealed significant positive spatial autocorrelation in the response
265 variables at fine spatial scales (within sites and in the 0-156 river km distance class), which
266 transitioned into significant negative correlation at intermediate distances (156-779 river km). In the
267 largest distance class (934-1,090 river km) autocorrelation was positive again. The selected
268 environmental variables accounted for most of the autocorrelation; the residuals of the environmental
269 RDA model were significantly correlated only within sites. The inclusion of spatial variables
270 successfully eliminated spatial autocorrelation in all distance classes.
271 The first canonical axis of the RDA ($R^2 = 0.409$, $df = 1$, $F = 152.7$, $P < 0.001$) separated *C.*
272 *curvispinum* from *C. sowinskyi*, placing *C. robustum* in an intermediate position (Fig. 4). On the
273 second axis ($R^2 = 0.181$, $df = 1$, $F = 67.6$, $P < 0.001$), however, *C. robustum* differentiated markedly
274 from the other two species. TSS showed the strongest correlation with the first axis among the
275 environmental variables (biplot scores: RDA1: -0.530, RDA2: 0.359), accounting mainly for the
276 separation of *C. curvispinum* from the other two species. Total nitrogen concentration pointed almost
277 exactly in the same direction as TSS; however, its effect was considerably weaker (RDA1: -0.157,

RDA2: 0.099). Current velocity (RDA1: -0.188, RDA2: -0.366) was associated mainly with *C. robustum*, whereas the centroids of substrate types concentrated around the origin of the ordination plane, indicating a relatively weak differentiation among the species in this regard.

The environmentally explainable variance fraction concentrated between river km 1,300 and 1,159 as a result of a peak in TSS coinciding with the absence of *C. sowinskyi* and *C. robustum* (Fig. 5a). The only spatially explainable part of the variance showed a complex distribution along the river with notable peaks in the Iron Gates section and in the vicinity of the delta (Fig. 5b).

Discussion

Our measurements revealed considerable differences in the filter mesh sizes among the invasive *Chelicorophium* species.. The relationship between filter mesh size and particle capture efficiency is not evident; particles smaller than the mesh size might be retained, especially when the material of the filter is sticky (Shimeta and Jumars 1991). Nevertheless, clearance rate dropped steeply for particles smaller than the mesh size in *Corophium volutator* (Pallas, 1766) (Møller and Riisgård 2006) in accordance with the particle size distribution of gut contents (Fenchel et al. 1975), suggesting that the primary filtering mechanism in corophiids is sieving (i.e. the mechanical retention of particles larger than mesh size of the filter; Shimeta and Jumars 1991). On the other hand, hydraulic resistance increases with smaller mesh sizes (Cheer and Koehl 1987), implying that less water can be filtered with the same effort; therefore, filters are not efficient at capturing particles considerably larger than the mesh size. Consequently, there is a particle size range for each species where their capture rate is higher than that of the others. Within this range, the species can tolerate a lower resource density than the others, translating into competitive advantage (Chase and Leibold 2003). Nevertheless, a sufficiently wide size distribution of the food particles might allow the coexistence of the species even locally, and spatial heterogeneity in resource availability also might promote their coexistence at the regional scale (Chase and Leibold 2003).

Accordingly,the interspecific differences in the filter mesh sizes among the invasive *Chelicorophium* species revealed in our study indicate niche differentiation by food particle size. Since spatial

differences were not detected over several hundred river km distances, our results can be considered as representative for the Lower Danube. Nevertheless, we expect that a similar pattern will be found wherever the three species coexist, and considerable differences will be observed only in situations where some of the species are missing, implying release from competitive pressure on the others.

Our study identified sources of variation in filter mesh size within the species, as well. The body length dependency of the character was marked in all three species, most likely reflecting ontogenetic changes. However, since repeated measurements on cohorts were not made in our study, alternative explanations (i.e. differences among cohorts) cannot be excluded with full certainty. Slight differences could be observed between genders, too, especially in *C. sowinskyi*. However, these are not likely to have ecological relevance; they might merely reflect the considerable sexual dimorphism in body proportions (i.e. males attain smaller standard lengths but have larger antennae). The ratio of unexplained variance in the models was also considerable, especially among and within the individuals of *C. curvispinum*, calling for further analyses.

Field data indicated the relevance of suspended matter in the niche differentiation among invasive Ponto-Caspian *Chelicorophium* species; the majority of the environmentally explained variance was attributable to this factor. Nevertheless, since only the overall quantity of suspended matter could be included in the analysis, its role is not trivial. As the morphological differences suggest, considerable explanatory power could be expected only from detailed data on the qualitative composition and size distribution of suspended particles. The effect of TSS was attributable mainly to the coincidence of peak values with the absence of *C. robustum* and *C. sowinskyi* in the Serbian river section (Fig. 5a). Since the downstream spread of *C. robustum* was still in progress at the time of the survey, its absence might not necessarily be the result of environmental factors. On the other hand, unfavorable suspended matter composition in this river section (combined with current velocity and sediment composition; Borza et al. 2015) could explain why the upstream distributional limit of the species used to be here for a long time. Recently, the species has been found at some additional sites in this river section (river km 1,334; Žganec et al., unpublished data); however, it is still early to draw conclusions in this question.

333 The distributional gap of *C. sowinskyi* was not related to any of the environmental factors included in
334 the analysis. However, former data show the eutrophic character of the river section downstream of
335 Budapest (Dokulil and Donabaum 2014), which might provide a historical explanation. The central
336 sewage treatment plant of the city began to operate only in 2010, so the species might not have had the
337 time to respond to the changed conditions at the time of the survey. Its record downstream of the city
338 might be an indication of its incipient spread (Borza et al. 2015).
339 High suspended matter load, however, does not necessarily lead to *C. curvispinum* dominance; the
340 extreme high density of *C. sowinskyi* downstream of the River Jantra mouth might be related to the
341 high TSS values in this tributary (125 mg/l during the survey). Unfortunately, TSS was measured at
342 only one point per site in the middle of the channel during the survey, so the connection is not
343 reflected in the data. Nevertheless, the peak densities recorded during the survey are still well below
344 the values recorded in the eutrophic River Rhine shortly after the invasion of *C. curvispinum* (up
345 to 750,000 ind./m^2; Van den Brink et al. 1993). The generally low density values of *Chelicorophium*
346 species and their strong response to the extra suspended matter load of tributaries suggest strong food
347 limitation in most parts of the Danube at the present time.
348 The explanatory power of the remaining variables was rather low; therefore, our field data do not
349 provide firm evidence for their importance in the niche differentiation of invasive *Chelicorophium*
350 species. The weak effect of total nitrogen concentration could not be separated from that of TSS, and
351 current velocity as well as substrate types also might be related to food availability, so they might not
352 necessarily represent independent niche axes. On the contrary, we assume that the larger body size of
353 *C. robustum* might be relevant to the coexistence of the species. In this case, various factors might be
354 potentially involved, including microhabitat use, generation time, predation risk, or interference
355 competition. Nevertheless, these can be expected only to modulate, not to overcome the differentiation
356 by food particle size.
357 In summary, differences in their filter mesh sizes allow a stable coexistence among the three invasive
358 *Chelicorophium* species, where their abundance is primarily determined by the quantity, quality, and
359 size distribution of suspended matter. Consequently, the joint impact of the three species – as
360 compared to *C. curvispinum* alone – is a more effective resource utilization, resulting in a stronger

benthic-pelagic coupling. Inferring from their smaller filter mesh sizes, the impact of the two recent invaders can be expected to be most pronounced if suspended matter is dominated by relatively small (< ~10 μm) food particles. It would be useful to compare invasive and presently non-invasive *Chelicorophium* species, which could provide insight into the factors of invasion success and allow a more accurate assessment of future invasion risks within the genus (Borza et al. 2017b). Similarly, to obtain a more complete overview about the utilization of suspended matter in the ecosystems concerned, it would be important to study all co-occurring filter feeding species jointly.

References

Altermatt F, Alther R, Fišer C, Jokela J, Konec M, Küry D, Mächler E, Stucki P, Westram AM (2014) Diversity and distribution of freshwater amphipod species in Switzerland (Crustacea: Amphipoda). PloS One 9:e110328

Atkinson CL, Vaughn CC, Forshay KJ, Cooper JT (2013) Aggregated filter-feeding consumers alter nutrient limitation: consequences for ecosystem and community dynamics. Ecology 94:1359–1369

Bernauer D, Jansen W (2006) Recent invasions of alien macroinvertebrates and loss of native species in the upper Rhine River, Germany. Aquat Invasions 1:55–71

Bernerth H, Dorow S (2010) *Chelicorophium sowinskyi* (Crustacea, Amphipoda) ist aus der Donau in den Main vorgedrungen - Anmerkungen zur Verbreitung und Morphologie der Art. Lauterbornia 70:53–71

Bernerth H, Tobias W, Stein S (2005) Faunenwandel im Main zwischen 1997 und 2002 am Beispiel des Makrozoobenthos. In: Faunistisch-ökologische Untersuchungen des Forschungsinstitutes Senckenberg im hessischen Main. Hessisches Landesamt für Umwelt und Geologie, Wiesbaden, pp 15–87

386 Bij de Vaate A, Jażdżewski K, Ketelaars HAM, Gollasch S, Van der Velde G (2002) Geographical
387 patterns in range extension of Ponto-Caspian macroinvertebrate species in Europe. Can J Fish
388 Aquat Sci 59:1159–1174

389 Blanchet FG, Legendre P, Borcard D (2008a) Modelling directional spatial processes in ecological
390 data. Ecol Model 215:325–336

391 Blanchet FG, Legendre P, Borcard D (2008b) Forward selection of explanatory variables. Ecology
392 89:2623–2632

393 Blanchet FG, Legendre P, Maranger R, Monti D, Pepin P (2011) Modelling the effect of directional
394 spatial ecological processes at different scales. Oecologia 166:357–368

395 Borza P (2011) Revision of invasion history, distributional patterns, and new records of Corophiidae
396 (Crustacea: Amphipoda) in Hungary. Acta Zool Acad Sci Hung 57:75–84

397 Borza P, Csányi B, Huber T, Leitner P, Paunović M, Remund N, Szekeres J, Graf W (2015)
398 Longitudinal distributional patterns of Peracarida (Crustacea, Malacostraca) in the River
399 Danube. Fundam Appl Limnol 187:113–126

400 Borza P, Csányi B, Paunović M (2010) Corophiids (Amphipoda, Corophioidea) of the River Danube
401 The Results of a Longitudinal Survey. Crustaceana 83:839–849

402 Borza P, Huber T, Leitner P, Remund N, Graf W (2017a) Current velocity shapes co-existence
403 patterns among invasive *Dikerogammarus* species. Freshw Biol 62:317–328

404 Borza P, Huber T, Leitner P, Remund N, Graf W (2017b) Success factors and future prospects of
405 Ponto–Caspian peracarid (Crustacea: Malacostraca) invasions: Is “the worst over”? Biol
406 Invasions 19:1517–1532

407 Brönmark C, Malmqvist B (1982) Resource partitioning between unionid mussels in a Swedish lake
408 outlet. Ecography 5:389–395

409 Chase JM, Leibold MA (2003) Ecological niches: linking classical and contemporary approaches.
410 University of Chicago Press, Chicago and London

411 Cheer AYL, Koehl MAR (1987) Paddles and rakes: fluid flow through bristled appendages of small
412 organisms. J Theor Biol 129:17–39

413 Dokulil MT, Donabaum U (2014) Phytoplankton of the Danube river: Composition and long-term
414 dynamics. Acta Zool Bulg Suppl 7:147–152

415 Fenchel T, Kofoed LH, Lappalainen A (1975) Particle size-selection of two deposit feeders: the
416 amphipod *Corophium volutator* and the prosobranch *Hydrobia ulvae*. Mar Biol 30:119–128

417 Forcellini M (2012) First record of the Ponto-Caspian invasive crustacean *Chelicorophium sowinskyi*
418 (Martinov, 1924) (Amphipoda, Corophiidae) in the French Rhône River. Crustaceana
419 85:1781–1785

420 Griffiths JR, Kadin M, Nascimento FJA, Tamelander T, Törnroos A, Bonaglia S, Bonsdorff E,
421 Brüchert V, Gårdmark A, Järnström M, Kotta J, Lindegren M, Nordström MC, Norkko A,
422 Olsson J, Weigel B, Žydelis R, Blenckner T, Niiranen S, Winder M (2017) The importance of
423 benthic-pelagic coupling for marine ecosystem functioning in a changing world. Glob Change
424 Biol 23: 2179–2196

425 Hellmann C, Worischka S, Mehler E, Becker J, Gergs R, Winkelmann C (2015) The trophic function
426 of *Dikerogammarus villosus* (Sowinsky, 1894) in invaded rivers: a case study in the Elbe and
427 Rhine. Aquat Invasions 10:385–397

428 Hering D, Moog O, Sandin L, Verdonschot PF (2004) Overview and application of the AQEM
429 assessment system. Hydrobiologia 516:1–20

430 Higgins SN, Vander Zanden MJ (2010) What a difference a species makes: a meta–analysis of
431 dreissenid mussel impacts on freshwater ecosystems. Ecol Monogr 80:179–196

Jones LA, Ricciardi A (2005) Influence of physicochemical factors on the distribution and biomass of invasive mussels (*Dreissena polymorpha* and *Dreissena bugensis*) in the St. Lawrence River. Can J Fish Aquat Sci 62:1953–1962

Kang C-K, Choy EJ, Hur Y-B, Myeong J-I (2009) Isotopic evidence of particle size-dependent food partitioning in cocultured sea squirt *Halocynthia roretzi* and Pacific oyster *Crassostrea gigas*. Aquat Biol 6:289–302

Kelleher B, Bergers PJM, Van den Brink FWB, Giller PS, Van der Velde G, Bij de Vaate A (1998) Effects of exotic amphipod invasions on fish diet in the Lower Rhine. Arch Für Hydrobiol 143:363–382

Labat F, Piscart C, Fontan B (2011) First records, pathways and distributions of four new Ponto-Caspian amphipods in France. Limnologica 41:290–295

Lefcheck JS (2016) piecewiseSEM: Piecewise structural equation modelling in r for ecology, evolution, and systematics. Methods Ecol Evol 573–579

Legendre P, Gallagher ED (2001) Ecologically meaningful transformations for ordination of species data. Oecologia 129:271–280

Legendre P, Legendre LF (2012) Numerical ecology. 3rd English edition. Elsevier, Amsterdam

Lesser MP, Shumway SE, Cucci T, Smith J (1992) Impact of fouling organisms on mussel rope culture: interspecific competition for food among suspension-feeding invertebrates. J Exp Mar Biol Ecol 165:91–102

Møller LF, Riisgård HU (2006) Filter feeding in the burrowing amphipod *Corophium volutator*. Mar Ecol Prog Ser 322:213–224

Nakagawa S, Schielzeth H (2013) A general and simple method for obtaining R^2 from generalized linear mixed-effects models. Methods Ecol Evol 4:133–142

455 Noordhuis R, van Schie J, Jaarsma N (2009) Colonization patterns and impacts of the invasive
456 amphipods *Chelicorophium curvispinum* and *Dikerogammarus villosus* in the IJsselmeer area,
457 The Netherlands. Biol Invasions 11:2067–2084

458 Oksanen J, Blanchet FG, Kindt R, Legendre P, Minchin PR, O'Hara RB, Simpson GL, Solymos P,
459 Stevens MHH, Wagner H (2017) vegan: Community Ecology Package. R package version
460 2.4-3. http://CRAN.R-project.org/package=vegan

461 Pinheiro J, Bates D, DebRoy S, Sarkar D, R Core Team (2016) nlme: Linear and Nonlinear Mixed
462 Effects Models. R package version 3.1-125, http://CRAN.R-project.org/package=nlme.

463 R Core Team (2016) R: A language and environment for statistical computing. R Foundation for
464 Statistical Computing, Vienna, Austria. URL http://www.R-project.org/

465 Riisgård HU, Larsen PS (2010) Particle capture mechanisms in suspension-feeding invertebrates. Mar
466 Ecol Prog Ser 418:255–293

467 Rohlf FJ (2015) tpsDig, Digitize Landmarks and Outlines, version 2.22. Department of Ecology and
468 Evolution, State University of New York, Stony Brook.

469 Shimeta J, Jumars PA (1991) Physical mechanisms and rates of particle capture by suspension-
470 feeders. Oceanogr Mar Biol - Annu Rev 29:l–257

471 Sousa R, Novais A, Costa R, Strayer DL (2014) Invasive bivalves in fresh waters: impacts from
472 individuals to ecosystems and possible control strategies. Hydrobiologia 735:233–251

473 Svensson JR, Marshall DJ (2015) Limiting resources in sessile systems: food enhances diversity and
474 growth of suspension feeders despite available space. Ecology 96:819–827

475 Van den Brink FWB, Van der Velde G, Bij de Vaate A (1993) Ecological aspects, explosive range
476 extension and impact of a mass invader, *Corophium curvispinum* Sars, 1895 (Crustacea:
477 Amphipoda), in the Lower Rhine (The Netherlands). Oecologia 93:224–232

478 Van der Velde G, Paffen BGP, Van den Brink FWB, Bij de Vaate A, Jenner HA (1994) Decline of
479 zebra mussel populations in the Rhine. Naturwissenschaften 81:32–34

480 Van Riel MC, Van der Velde G, Rajagopal S, Marguillier S, Dehairs F, Bij de Vaate A (2006) Trophic
481 relationships in the Rhine food web during invasion and after establishment of the Ponto-
482 Caspian invader *Dikerogammarus villosus*. Hydrobiologia 565:39–58

483 Wallace JB, Webster JR, Woodall WR (1977) The role of filter feeders in flowing waters. Arch Für
484 Hydrobiol 79:506–532

485 Zhang X, Liu Z, Jeppesen E, Taylor WD, Rudstam LG (2016) Effects of benthic-feeding common
486 carp and filter-feeding silver carp on benthic-pelagic coupling: implications for shallow lake
487 management. Ecol Eng 88:256–264

488 Zuur AF, Ieno EN, Walker NJ, Saveliev AA, Smith GM (2009) Mixed effects models and extensions
489 in ecology with R, Springer Science and Business Media. New York

490

491 **Tables**

492

493 **Table 1** Number of specimens involved in the morphometric measurements. *C. robustum* was divided

494 into two size classes due to the non-linear body length dependence of its filter mesh size (see text)

Species	river km 532	river km 375	river km 104	Σ
C. curvispinum		23 (9 ♂, 13 ♀, 1 juv.)	13 (7 ♂, 6 ♀)	36
C. robustum (< 5.5 mm)		15 (6 ♂, 7 ♀, 2 juv.)	8 (3 ♂, 5 ♀)	23
C. robustum (≥ 5.5 mm)		11 (3 ♂, 8 ♀)	2 (2 ♀)	13
C. sowinskyi	20 (9 ♂, 10 ♀, 1 juv.)		10 (5 ♂, 5 ♀)	30

495

496 **Table 2** Definitions of substrate types used in the study

497

Substrate type	Definition
riprap	rocks of variable size, artificial
macrolithal	blocks, large cobbles; grain size 20 cm to 40 cm
mesolithal	cobbles; grain size 6 cm to 20 cm
microlithal	coarse gravel; grain size 2 cm to 6 cm
akal	fine to medium-sized gravel; grain size 0.2 cm to 2 cm
psammal	sand; grain size 0.063-2 mm
psammopelal	sand and mud
pelal	mud (organic); grain size < 0.063 mm
argyllal	silt, loam, clay (inorganic); grain size < 0.063 mm
macrophytes	submerged macrophytes, including moss and Characeae
xylal	tree trunks, dead wood, branches, roots

498

499 **Table 3** Parameters and variance components of the single-species linear mixed-effects models

500

Species	Intercept (μm)	Slope (body length)	Body length-dependency (= fixed effects)	Among-individual variation (= random effects)	Within-individual variation (= residual)
C. curvispinum	7.51 (*SE* = 1.42; *P* < 0.001)	1.02 (*SE* = 0.40; *P* = 0.015)	0.15	0.80	0.05
C. robustum (< 5.5 mm)	5.02 (*SE* = 0.64; *P* < 0.001)	0.92 (*SE* = 0.16; *P* < 0.001)	0.41	0.27	0.32
C. robustum (≥ 5.5 mm)	9.90 *(SE* = 0.08; *P* < 0.001)	not significant	-	0.11	0.89
C. sowinskyi	1.77 (*SE* = 0.45; *P* < 0.001)	0.83 (*SE* = 0.14; *P* < 0.001)	0.52	0.44	0.04

Figure captions

Fig. 1 Occurrences of *Chelicorophium* species in the River Danube during Joint Danube Survey 3 (multi-habitat samples only). White squares: *C. curvispinum*, grey circles: *C. sowinskyi*, black triangles: *C. robustum*. The dark shaded area corresponds to the River Danube basin. Codes of the riparian countries: DE: Germany, AT: Austria, SK: Slovakia, HU: Hungary, HR: Croatia, RS: Serbia, RO: Romania, BG: Bulgaria, MD: Moldova, UA: Ukraine

Fig. 2 Filter mesh sizes of *Chelicorophium* species as a function of body length. Lines represent the fitted values of the single-species linear mixed-effects models

Fig. 3 Mantel correlograms of the response variables, the residuals of the environmental model (E), and the residuals of the environmental and spatial model (E + S). The distance class at 0 river km corresponds to within-site distances. Solid symbols indicate significant correlations (*: $P < 0.05$, **: $P < 0.01$, ***: $P < 0.001$). Numbers on the top of the graph indicate the number of pairs involved in the calculation of correlations for each distance class. Symbols are connected only to visualize the trends

Fig. 4 Triplot showing the results of the RDA including both environmental and spatial explanatory variables ('*WA*' scores, species scaling). Cc: *C. curvispinum*, Cs: *C. sowinskyi*, Cr: *C. robustum*. Substrate types: AKA: akal, ARG: argyllal, MAL: macrolithal, MEL: mesolithal, MIL: microlithal, MPH: macrophytes, PEL: pelal, PPE: psammopelal, PSA: psammal, RIP: rip-rap, XYL: xylal. Arrows represent continuous environmental variables (cur: current velocity, tss: total suspended solids, toN: total nitrogen). AEM eigenfunctions are not shown for the sake of perspicuity

Fig. 5 The distribution of the environmentally (a) and the only spatially (b) explainable part of variance (i.e. the fitted site scores of the first canonical axis in the corresponding RDA models) along the investigated river section. Solid lines represent smoothed splines (function 'smooth.spline' in R)

528 with a smoothing parameter of 0.5. Total suspended solid (TSS) values are shown in (a) for

529 comparison

530 Figures

531 Fig. 1

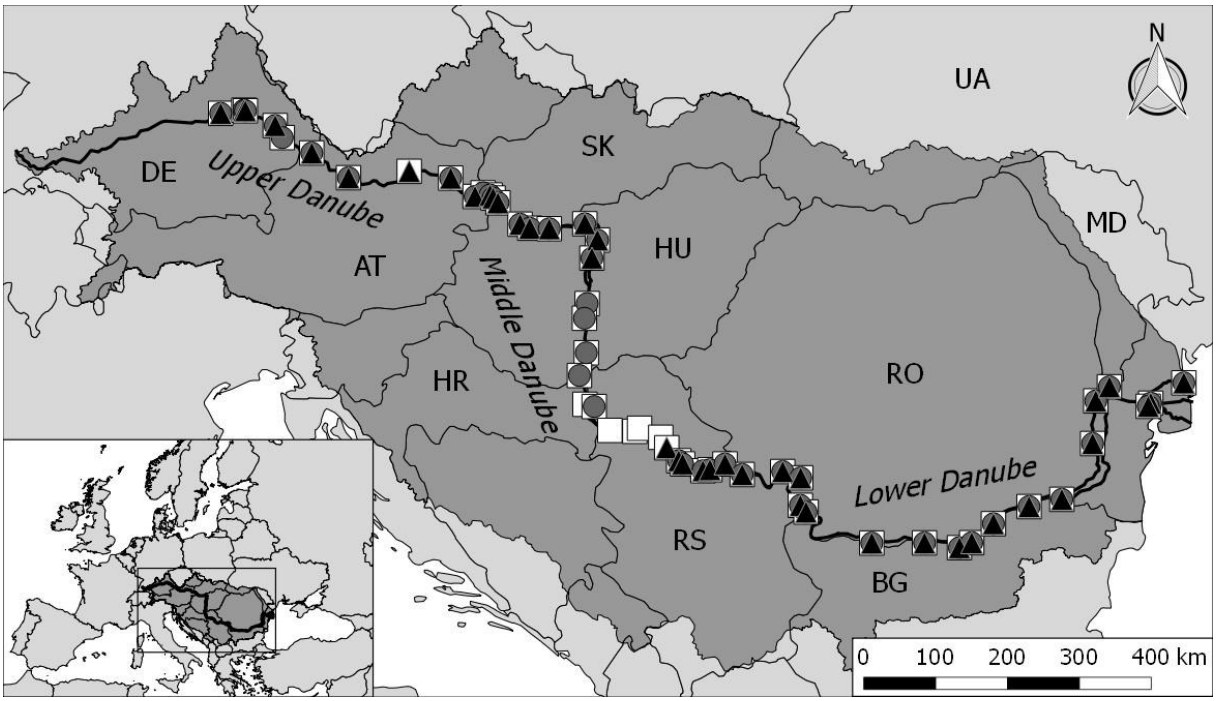

532

533 Fig. 2

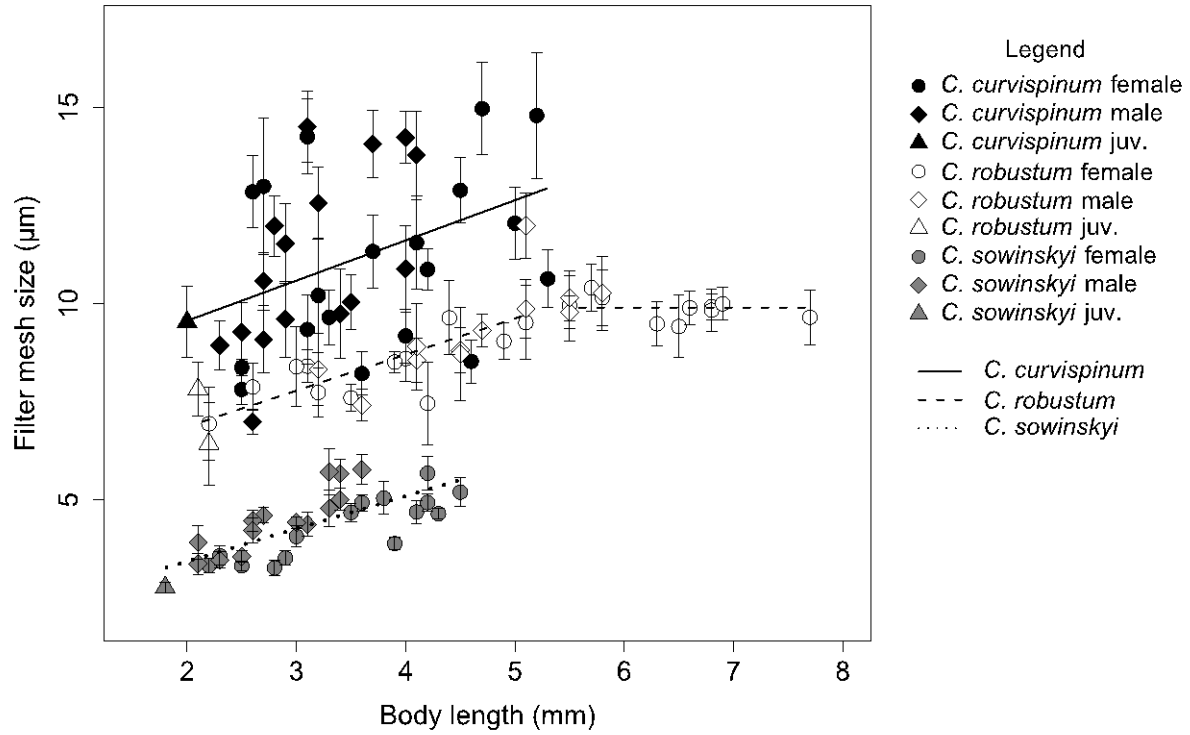

534

535 Fig. 3

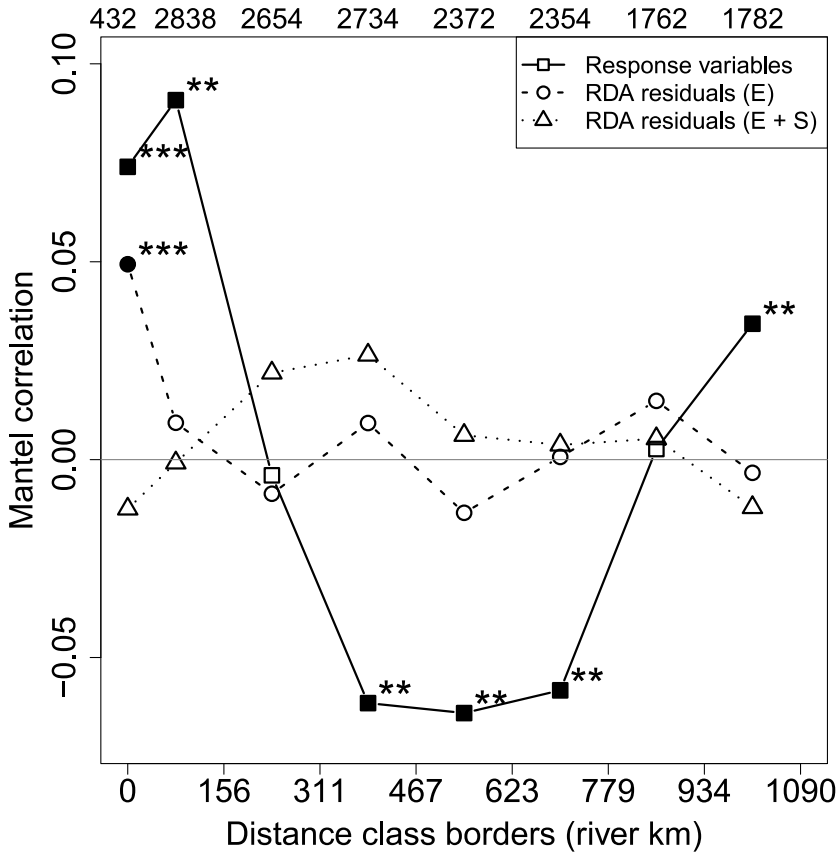

536

537 Fig. 4

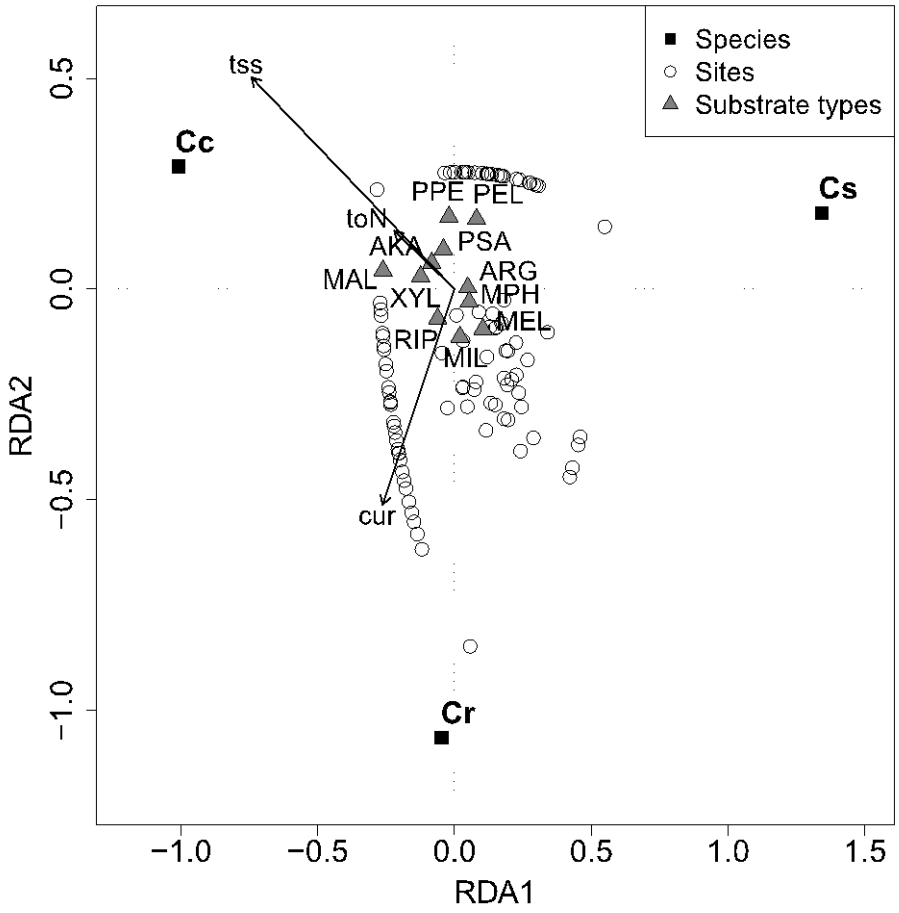

538

539 Fig. 5

a

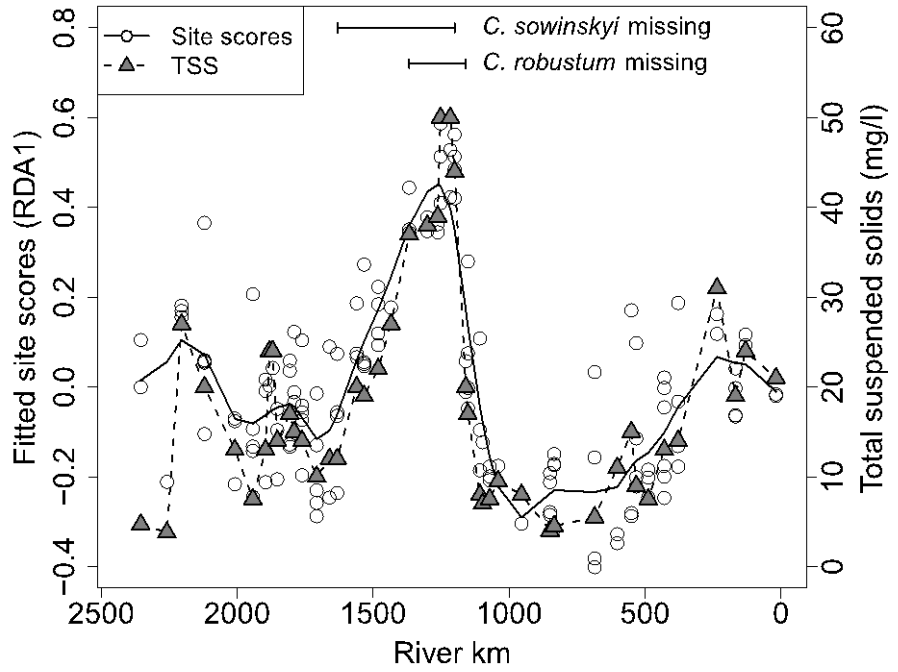
Site scores
TSS
C. sowinskyi missing
C. robustum missing
Fitted site scores (RDA1)
Total suspended solids (mg/l)
River km

b

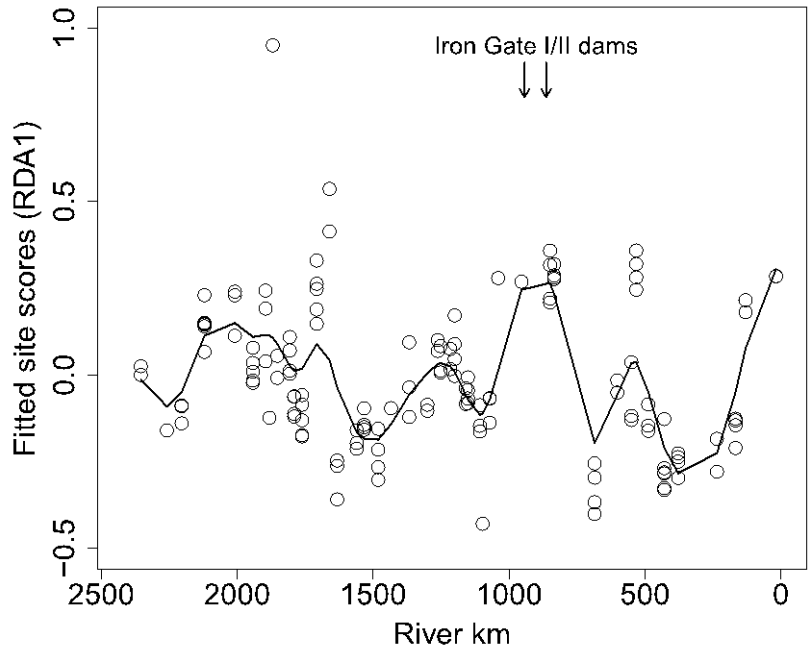
Iron Gate I/II dams
Fitted site scores (RDA1)
River km

540